Measurement of Oil-Water Flows by Conductance Cross-Correlation Flowmeter with Center Body in a Small Pipe

L. D. Bai, N. D. Jin*， W. K. Ren, Z. Y. Tang, C. S. Liu

School of Electrical and Information Engineering, Tianjin University, Tianjin, China
E-mail (Ningde Jin): ndjin@tju.edu.cn

Abstract

Accurate measurement of oil-water flows is a significant issue to oilfield water injection development. In this paper, the parameter measurement of vertical oil-water flows is established by conductance sensors with inner-outer multi-height ring electrodes. Firstly, the dynamic experiment of vertical upward oil-water flows is carried out, and a high-speed camera is used to capture flow structures in each working condition. Based on the output conductance signals and the images from the high-speed camera, the experimental flow patterns (bubble flow, slug flow, very fine bubble flow and transition flow) are identified. And the relationship of mixture velocity to cross-correlation velocity and water cut is established. On this basis, the drift velocity models under different flow patterns are constructed by combining the water holdup calculated by Maxwell equation. The results show that the measurement of mixture velocity of oil-water flows is satisfactory. And high precision superficial velocity measurements of four different flow patterns are achieved.

1. Introduction

The phenomenon of oil-water flows is commonly encountered in petroleum industry. In particular, accurate flow measurement of oil-water flows is significant to dynamic characteristics of oil well production. For the water continuous oil-water flow with low velocity, due to the interaction and slippage effect among phases, the flow structure is very complex, and the local distributions of velocity and concentration are extremely inhomogeneous, which bring a great challenge to the flow measurement.

The traditional electric methods for the measurement of oil-water flows include conductance method, capacitance method and so on. The conductance method has the advantages of fast response, good reproducibility and satisfied stability which is suitable for multi-phase flow measurement with water as continuous phase. Common conductance sensors include probe array structure [1-6], sector structure [7, 8], ring structure, parallel string wire, wire-mesh and so on. In order to improve the electric field distribution of the sector sensor, rotating electric field type conductance sensor [9-11] and multi-sector conductance sensor [12, 13] were designed, which further improve the sensitivity of water holdup measurement as well as inhibit the influence of flow structure in some way. To explore the concentration distribution of the fluid corresponding to the pipe cross section, researchers began to introduce annular conductance sensors [14-16]. In addition, the measurement of flow velocity is the key to obtain the flow rate of oil-water flows. In long-term experiments and engineering studies, the flow velocity measurement methods mainly include Venturi flowmeter, turbine flowmeter and cross-correlation flowmeter et al. [17-19]. In the process of water injection development in onshore oilfield, the phenomenon of oil-water flows with water as continuous phase gradually increases, and the conductance cross-correlation method is widely used to measure flow velocity [20-22]. The purpose of cross-correlation measurement is to obtain the mixture velocity of the fluid through the cross-correlation velocity which reflects the propagation velocity of structural wave from upstream sensor to downstream sensor. However, some conductance sensors only can reflect the propagation velocity of local structural wave, rather than that of global structural wave which has adverse effect on the velocity measurement of serious non-uniform oil-water flows. Besides, the traditional flow measurement often relies on a combination of water holdup sensor and velocity sensor, which in fact increases the cost.

Based on this, we report an experimental study on flow measurement of vertical upward oil-water flows using conductance sensor with inner-outer multi-height ring electrodes, which is designed and used in the study of gas-liquid flow [23] by our group. In the dynamic experiment, four flow patterns are identified by combining images of high-speed camera and the output signals. Simultaneously, the cross-correlation velocity is attained by the principle of cross-correlation velocity, then the mixture velocity is established based on the cross-correlation velocity and water cut. In addition, we calculate the water holdup with the Maxwell equation. Finally, drift velocity models based on four flow patterns is constructed to acquire superficial velocities.

2. Experiment setup

2.1 Sensor system

In this paper, the water holdup and mixture velocity of vertical oil-water flows are measured by improved ring conductance sensor. The sensor structure is shown in Fig. 1. The sensor consists of an exciting ring electrode on the center body and a receiving ring electrode embedded in the pipe wall, which can be used to measure water holdup. In addition, two identical conductance sensors are placed upstream and downstream of the measurement section for the measurement of cross-correlation velocity.

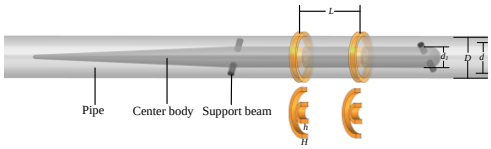

Figure 1: Structure of the conductance sensor with inner-outer multi-height ring electrodes

Table 1: The geometry of conductance sensor

Key parameters	Letters	Values
Inner diameter of the pipe	d	20 mm
Outer diameter of the pipe	D	30 mm
Diameter of the center body	d_1	10 mm
Inner electrode height	h	4 mm
Outer electrode height	H	3 mm
Distance between the upstream and downstream electrodes	L	30 mm

The COMSOL software was used to optimize the dimension of the sensor, and the optimal sensor structure with the highest measurement sensitivity, the most uniform electric field distribution and good measurement stability was finally obtained, as shown in Tab. 1. We have explained the specific optimization design process of the sensor in literature [23]. The design of unequal height electrodes ensures the uniform distribution of electric field in annular space, which is beneficial to overcome the influence of uneven distribution of the dispersed phase on water holdup measurement. The distance between the sensors is 30 mm, which ensures the independent measurement of the two sensors and effectively avoids the electric field crosstalk between the two sensors. The excitation source of the sensor is a 20 kHz sinusoidal AC voltage source with a peak value of 10 V, the two inner ring electrodes are excited respectively, and the sensor signals received by the outer ring electrodes are subsequently amplified, filtered, AD converted. Finally, the signals are collected by PXI-4472, and then processed by the upper computer.

2.2 Dynamic experiment

The dynamic experiment of vertical upward oil-water flows is carried out in the multiphase flow loop device of Tianjin University, as shown in Fig. 2. It mainly includes three tanks: water tank, oil tank and mixing tank; high-precision peristaltic pump with stable and reliable performance; PMMA (polymethyl methacrylate) experimental pipes with length of 2600 mm, inner diameter of 20 mm and outer diameter of 30 mm; The conductance sensor and measurement system. The water phase of the fluid is tap water at room temperature, and the oil phase is No. 3 industrial white oil (density is 801 kg/m^3, viscosity is 2.8 mPa·s). The actual total flow Q_m and water cut K_w can be obtained through the peristaltic pump. Before each experiment, the pump is calibrated to ensure a same initial value of each working condition. A high-speed camera is used to capture the flow structure which is installed 150 cm above the vertical pipe entrance. The distance can ensure the fluid fully developed prior to measurement. After measurement, the fluid eventually flows into the mixing tank for separation to use again. In the experiment, the total flow Q_m of oil-water flows varies from 2 m^3/d-9 m^3/d, corresponding mixture velocity U_m range of 0.073 m/s-0.332 m/s, and the water cut varies from 50% to 100%.

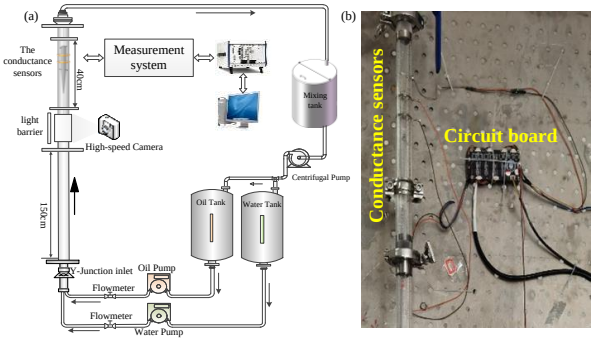

Figure 2: The experiment setup: (a) schematic diagram of the experimental oil-water flow loop; (b) sensor system.

2.2 Flow patterns

According to the images taken by high-speed camera, four oil-water flow patterns can be observed in the experiment: Very fine bubble flow, bubble flow, slug flow and transition flow, as shown in Fig. 3. When Q_m is low, the slippage between oil and water phases is significant, therefore, the small oil bubbles tend to coalesce and form large oil slugs, and most of oil slugs are located in the pipe center. What's more, there are a certain number of oil bubbles below oil slugs, which form the tail structure. In this case, the corresponding oil-water flow pattern is slug flow (Fig.3 (a)). With the increase of Q_m, the turbulent kinetic energy of the mixed fluid gradually increases, and bubble flow occurs (Fig.3 (b)). At this time, large oil slugs are broken into smaller oil bubbles. In addition, the number of oil bubbles in the pipe is gradually increased and the diameter of oil bubbles is various, resulting in a complex flow behavior. With the further increase of Q_m, the oil bubbles are further broken into very fine ones under the condition of extremely high water cut, and the flow pattern of oil-water two-phase flow evolves into very fine bubble flow (Fig.3 (c)). When K_w is low and Q_m is high, transition flow appears (Fig.3 (d)). Alternating flow structures with oil as the continuous phase and water as the continuous phase are obtained. When the oil phase is continuous, large water bubbles appear in the pipe, but the duration of the continuous oil phase is very short. When water is a continuous phase, the oil phase flows upward in the center of the pipe in quasi-slug structures, while the water

phase is distributed in the local area of the pipe and contains a certain number of oil bubbles.

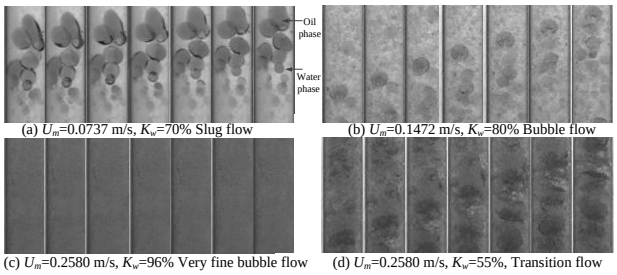

(a) U_m=0.0737 m/s, K_w=70% Slug flow (b) U_m=0.1472 m/s, K_w=80% Bubble flow

(c) U_m=0.2580 m/s, K_w=96% Very fine bubble flow (d) U_m=0.2580 m/s, K_w=55%, Transition flow

Figure. 3: Snapshots of experimental flow patterns captured by a high speed camera in vertical oil-water two-phase flow pipes

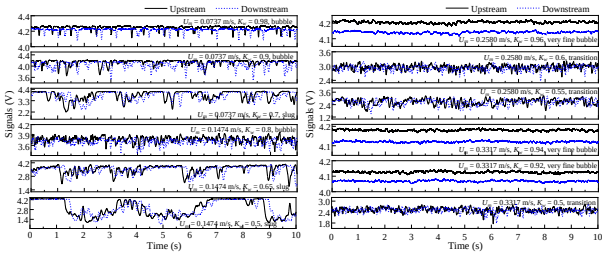

Figure 4: The output signals from the conductance sensor with inner-outer multi-height ring electrodes

The output signals of the conductance sensors are shown in Fig. 4. For slug flow, the output signal shows the characteristic of alternating high level and low level periodically. The small fluctuation of the high-level signal indicates the existence of small oil bubbles in the continuous water phase, and the small fluctuation of the low-level signal indicates the influence of the liquid film on the part of the oil slug. For bubble flow, a large number of downward spikes appear in the measured signals, and the distribution is approximately random and uniform. For very fine bubble flow, the uniform distribution of the fluid makes the fluctuation of output signal very small. For transition flow, due to the increase of oil phase, the output voltage is reduced, and has a periodicity similar to that of slug flow, but the signal fluctuation frequency increases and the response time of oil slug is shorter. In addition, with the increase of total flow velocity and the decrease of water content, the signal fluctuation becomes more severe.

Based on the above analysis, the flow pattern map of oil-water flows is obtained as shown in Fig. 5. The horizontal axis and vertical axis represent the mixture velocity U_m and water cut K_w respectively. It can be seen that slug flow is basically located in the region of lower U_m. When the water cut exceeds 70%, the flow pattern gradually evolves to bubble flow with the increase of mixture velocity. VFD O/W occurs at the working conditions of high U_m and very high K_w. When the water cut is less than 65%, the transition flow pattern appears.

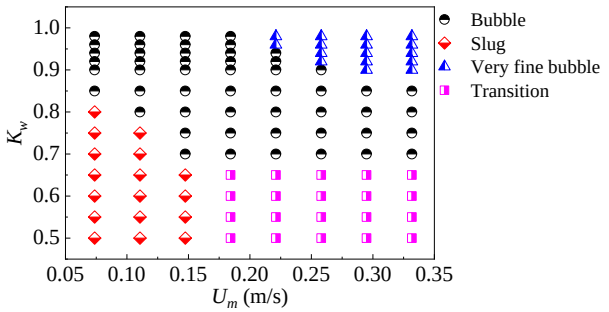

Figure 5: The flow pattern map of oil-water flows in vertical pipe.

3. Results and discussions

3.1 The mixture velocity of oil-water flows

The cross-correlation velocity of oil-water flows can be calculated based on the upstream and downstream sensor signals $x(t)$ and $y(t)$ [19]:

$$R_{xy}(\tau) = \lim_{N\to\infty} \frac{1}{N} \int_0^N x(t)y(t+\tau)dt \tag{1}$$

where N is the integration time, and the transit time τ_0 corresponds to the τ for max $R_{xy}(\tau)$, and the cross-correlation velocity is $U_{cc} = L/\tau_0$. L is the distance between upstream and downstream sensors.

In order to make the measurement accuracy of U_{cc} higher, appropriate sample frequency should be adopted [23, 24]. In this experiment, the maximum U_m at the inlet of the pipe is 0.33 m/s, and the velocity through the annular space of the center body is not more than 0.44 m/s. To ensure that the maximum relative error caused by the measurement frequency does not exceed 0.05%, the sample frequency is determined as 20 kHz.

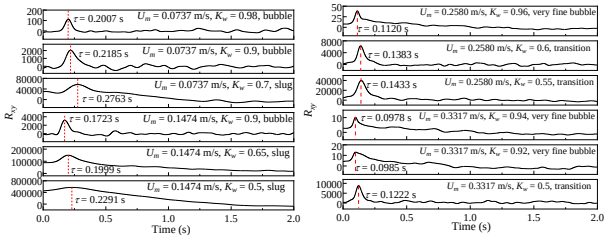

Figure 6: The cross-correlation functions based on the signals from conductance sensors with inner-outer multi-height ring electrodes under typical oil-water flow conditions

The calculation results of cross-correlation method are shown in Fig. 6. It shows that there is a satisfactory correlation between two sensors indicating that the flow structure between the two sensors keeps the same. And the introduction of the center body effectively weakens the influence of non-uniform distribution of the fluid. Fig. 7(a) shows the calculation results of U_{cc}, similar to gas-liquid flow [23], for the same U_m, the transit time increases with the decrease of water cut, leading to a decrease of U_{cc}. For the same water cut, the transit time decreases with the increase of U_m, resulting in the

increase of U_{cc}. And the change rule of U_{cc} under different flow patterns tends to be consistent, indicating that the conductance sensor has the ability to capture global structural waves of oil-water flows.

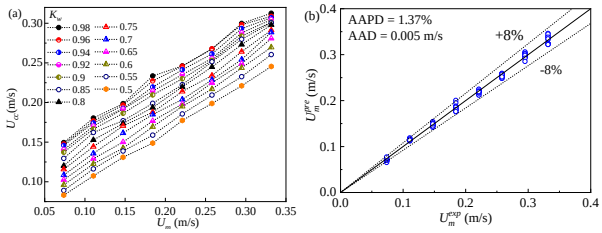

Figure 7: The measured cross-correlation velocity with inner-outer multi-height ring electrodes: (a) the cross-correlation velocity U_{cc} versus the mixture velocity U_m and water cut K_w; (b) the prediction accuracy of mixture velocity.

According to the research of Kytömaa and Brennen [25], the cross-correlation velocity U_{cc} is equal to the velocity of kinematic wave U_{kw}. But U_{kw} is not equal to the U_m of the fluid because of the slippage effect and the interaction between oil and water phases. In the study of bubbly oil-in-water flows, Lucas and Jin [26] found the following relationship of U_{kw} to the U_m and Y_o:

$$\begin{aligned} U_{cc} = U_{kw} &= C_{01}U_m + Y_o U_m \frac{dC_{01}}{dY_o} + U_\infty (1-Y_o)^{n-1}[1-Y_o(n+1)] \\ &= (C_{01} + Y_o \frac{dC_{01}}{dY_o})U_m + U_\infty (1-Y_o)^{n-1}[1-Y_o(n+1)] \\ &= C^* U_m + U^* \end{aligned} \tag{2}$$

where C_{01} represents the phase distribution coefficient, n is the droplet size exponent, and U_∞ the terminal velocity of a single droplet in infinite still water. Therefore, the relationship between U_{cc} and U_m is influenced by the phase distribution characteristic and oil content. According to the cross-correlation velocity in Fig. 7(a), for a fixed U_m, there is a linear increasing relationship between the cross-correlation velocity and the water cut. In this paper, C^* and U^* in Eq. (3) are linearly fitted in combination with water cut, and the mixture velocity U_m is finally obtained:

$$U_m = \frac{U_{cc} - (0.15278K_w - 0.0444)}{0.68712 - 0.04856K_w} \tag{3}$$

In order to evaluate the accuracy of the conductance sensor to the measurement of oil-water flows, two statistical indexes [23]: The absolute average percentage deviation (AAPD) and the absolute average deviation (AAD), are introduced in this paper. Fig. 7(b) shows the prediction result of mixture velocity under each working condition. We can see that the prediction results of U_m have high precision, basically within the total error line of ±8%, the AAPD of 1.37% and the AAD of 0.005 m/s.

3.2 Water holdup

The change of water holdup and flow structure will lead a variation of mixture conductivity of oil-water flows. For conductance sensors, Maxwell formula [27] can be used to calculate the holdup of dispersed phase according to changes in conductivity. For the oil-water flows in which water is the continuous phase, the dispersed phase is the oil phase, so the oil holdup Y_o can be calculated according to Maxwell formula:

$$\frac{\sigma_m - \sigma_w}{\sigma_m + 2\sigma_w} = Y_o \frac{\sigma_o - \sigma_w}{\sigma_o + 2\sigma_w} \tag{4}$$

where σ_o and σ_w are the conductivity of oil and water phases, respectively, and $Y_w = 1 - Y_o$. For the conductance sensor adopted in this paper, σ_m / σ_w can be expressed by the measured voltage, the apparent water holdup can be written as follows:

$$Y_w^* = \frac{3}{1 + 2/(\sigma_m / \sigma_w)} = \frac{3}{1 + 2\dfrac{V_{ref}^w \cdot V_m}{V_{ref} \cdot V_m^w}} \tag{5}$$

where V_{ref} is the voltage of the reference resistor, V_m is the output voltage of the sensor, V_m^w is the voltage corresponding to pure water.

Based on this, the calculation results of water holdup under different working conditions are shown in Fig. 8. It can be seen from the figure that, in general, the sensor has a good resolution in the measurement of water holdup under working conditions. When the U_m is low, large slippage between oil and water phases lead to greater Y_w compared with K_w. And when the K_w is low, the Y_w decreases with the increase of U_m. When the U_m exceeds 0.25 m/s, the slippage effect almost disappears. It is worth noting that when the K_w is greater than 90%, the measurement of Y_w is almost not affected by the U_m, which indicates that the sensor still has a good effect on the measurement of water holdup of oil-water flows with low-velocity and high water-cut. This is because the center body plays the role of collecting flow, which weakens the influence of uneven distribution of oil phase on water holdup measurement. In addition, the collecting effect also increases the turbulent kinetic energy of the fluid which increase the number of oil bubbles in the annular space, making Maxwell formula suitable for a wider range of water holdup measurement.

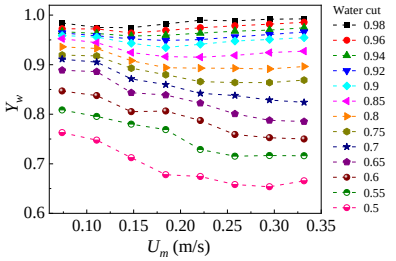

Figure 8: The response of water holdup in case of mixture velocity and water cut.

3.3. Superficial velocity of oil-water flows

After the water holdup and mixture velocity of oil-water flows are calculated, drift velocity models are proposed to predict the phase superficial velocity of oil-water flows. The drift-flux model is proposed by Zuber and Findlay [28] to study the slippage effect among incompatible fluids. For oil-water flows, the drift-flux model can be expressed as follows:

$$\frac{U_{so}}{Y_o\left(1-Y_o\right)^n}=C_0\frac{U_m}{(1-Y_o)^n}+U_\infty \tag{6}$$

Equation 6 shows that C_0 and U_∞ are the linear parameters of $U_{so}/Y_o(1\text{-}Y_o)^n$ and $U_m/(1\text{-}Y_o)^n$, which are influenced by flow patterns. Therefore, the drift velocity models based on different flow pattern are established in this paper, as shown in Fig. 9. For different flow patterns, appropriate droplet size exponent n is selected to obtain a satisfactory linear relationship between $U_{so}/Y_o(1\text{-}Y_o)^n$ and $U_m/(1\text{-}Y_o)^n$.

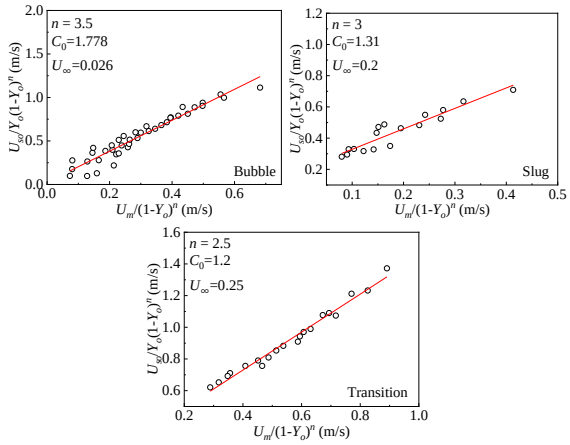

Figure 9: $U_{so}/Y_o(1\text{-}Y_o)^n$ versus $U_m/(1\text{-}Y_o)^n$ for different flow patterns

Therefore, the drift velocity models for three flow pattern can be expressed as follows:

$$\frac{U_{so}}{Y_o}=\begin{cases}1.778U_m+0.026(1-Y_o)^{3.5}, & \text{Bubble}\\ 1.31U_m+0.2(1-Y_o)^3, & \text{Slug}\\ 1.2U_m+0.25(1-Y_o)^{2.5}, & \text{Transition}\end{cases} \tag{7}$$

However, for very fine bubble flow, the slippage effect is very weak due to the large mixture velocity, and the oil phase is evenly distributed in the water phase of the pipe. When the drift velocity model is used to characterize the slippage, it is found that the error is very large. Therefore, we directly establish the relationship between Y_w and K_w. $K_w=1.8403Y_w-0.85$ can be obtained by linear fitting, the superficial velocity of oil phase for very fine bubble flow can be expressed by the following formula:

$$U_{so}=U_m(1-K_w)=U_m(1.85-1.84Y_w) \tag{8}$$

By substituting the phase holdup Y obtained by the conductance sensor system and U_m obtained by the cross-correlation method into Equations (7) and (8), the superficial velocities of oil and water phases under four different flow patterns can be obtained satisfactory, as shown in Fig. 10. The AAPD and the AAD of U_{so} are 1.67% and 0.0027 m/s, respectively, and those of U_{sw} are 1.6% and 0.0052 m/s. Compared with the four-sectors structure [13], the sensor structure renders the electric field distribution more uniform and improves the measurement sensitivity. In addition, compared with the combination of different sensors in references [6] and [21], the introduction of the center body of the sensor makes the effect of the sensor collector obvious, which leads to a wider measurement range of water content. Furthermore, in the measurement of oil-water flows with water as continuous phase, the sensor has achieved good measurement effect on the prediction of total velocity, superficial velocity and water holdup of four different flow patterns.

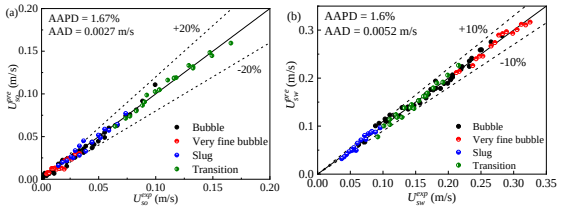

Figure 10: The prediction accuracy of superficial velocity of oil and water phases

4. Conclusion

In this paper, a conductance cross-correlation flowmeter with center body is used to measure the vertical upward oil-water flows in a 20 mm pipe. For the water continuous oil-water flows with low velocity, complex flow structure has great influence on flow measurement. Therefore, we first capture the flow pattern based on the dynamic experiments, four flow patterns under experimental conditions are identified. What's more, the drift velocity models under different flow patterns are constructed. The result shows that the conductance sensor structure renders the electric field distribution more uniform and improves the sensitivity of the measurement. Moreover, it can obtain both water holdup and mixture velocity of oil-water flow with high accuracy. The AAPD and the AAD of oil phase superficial velocity are 1.67% and 0.0027 m/s, respectively. And those of water phase superficial velocity are 1.6% and 0.0052 m/s. The conductance sensor is not only suitable for gas-liquid flow measurement but also achieves good flow measurement accuracy in oil-water flows.

Acknowledgments

This study was supported by National Natural Science Foundation of China (Grant No. 42074142, 51527805) and Tianjin Research Innovation Project for Postgraduate Students (2021YJSS020).

References

[1] Van Rossum J J, "Experimental investigation of horizontal liquid films: Wave formation, atomization, film thickness", *Chemical Engineering Science*, **11,** 35-52, 1959.

[2] Kelessidis V C, Dukler A E, "Modeling flow pattern transitions for upward gas-liquid flow in vertical concentric and eccentric annuli", *International Journal of Multiphase Flow*, **15**, 173-191, 1989.
[3] Brown R C, Andreussi P, Zanelli S, "The use of wire probes for the measurement of liquid film thickness in annular gas-liquid flows", *The Canadian Journal of Chemical Engineering*, **56**, 754-757, 1978.
[4] Barnea D, Shoham O, Taitel Y, "Flow pattern characterization for two phase flow by electrical conductance probe", *International Journal of Multiphase Flow*, **6**, 387-397, 1980.
[5] Koskie J E, Mudawar I, Tiederman W G, "Parallel-wire probes for measurement of thick liquid films", *International Journal of Multiphase Flow*, **15**, 521-530, 1989.
[6] Han Y F, Jin N D, Zhai L S, et al., "Flow pattern and holdup phenomena of low velocity oil-water flows in a vertical upward small diameter pipe", *Journal of Petroleum Science and Engineering*, **159**, 387-408, 2017.
[7] Costigan G, Whalley P B, "Slug flow regime identification from dynamic void fraction measurements in vertical air-water flows", International Journal of Multiphase Flow, **23**, 263-282, 1997.
[8] Song C H, Chung M K, No H C, "Measurements of void fraction by an improved multi-channel conductance void meter", *Nuclear Engineering and Design*, **184**, 269-285, 1998.
[9] Tournaire A, "Dependence of the instantaneous response of impedance probes on the local distribution of the void fraction in a pipe", *International Journal of Multiphase Flow*, **12**, 1019-1024, 1986.
[10] Rocha M S, Simões-Moreira J R, "Void fraction measurement and signal analysis from multiple-electrode impedance sensors", *Heat Transfer Engineering*, **29**, 924-935, 2008.
[11] Wang D Y, Jin N D, Zhuang L X et al., "Development of a rotating electric field conductance sensor for measurement of water holdup in vertical oil-gas-water flows", *Measurement Science and Technology*, **29**, 075301, 2018.
[12] Gao Z K, Yang Y Y, Zhai L S et al., "A four-sector conductance method for measuring and characterizing low-velocity oil-water two-phase flows", *IEEE Transactions on Instrumentation and Measurement*, **65**, 1690-1697, 2016.
[13] Bai L D, Jin N D, Chen X, et al., "A distributed conductance cross-correlation method for measuring low-velocity and high water-cut oil-water flows", *IEEE Sensors Journal*, **21**, 23860-23871, 2021.
[14] Asali J C, Hanratty T J, Andreussi P, "Interfacial drag and film height for vertical annular flow", *AIChE Journal*, **31**, 895-902, 1985.
[15] Lucas G P, Cory J C, Waterfall R C, "A six-electrode local probe for measuring solids velocity and volume fraction profiles in solids-water flows", *Measurement Science and Technology*, **11**, 1498-1509, 2000.
[16] Jin N D, Zhao X, Wang J et al., "Design and geometry optimization of a conductivity probe with a vertical multiple electrode array for measuring volume fraction and axial velocity of two-phase flow", *Measurement Science and Technology*, **19**, 045403, 2008.
[17] Xu L, Zhou W, Li X, Wang M, "Wet-gas flow modeling for the straight section of throat-extended venturi meter", *IEEE Transactions on Instrumentation and Measurement*, **60**, 2080-2087, 2011.
[18] Li D H, Feng F F, Wu Y X et al., "Investigation of the mixture flow rates of oil-water two-phase flow using the turbine flow meter", *Journal of Physics Conference*, **10**, 1088, 2009.
[19] Beck M S, "Correlation in instruments: cross correlation flow meters", *Journal of Physics E: Scientific Instruments*, **14**, 7-19, 1981.
[20] Thorn R, Beck M S, Green R G, "Non-intrusive methods of velocity measurement in pneumatic conveying", *Journal of Physics E: Scientific Instruments.* **15,** 1131-1139, 1982.
[21] Wang D Y, Jin N D, Zhai L S et al., Methodology for production logging in oil-in-water flows under low flow rate and high water-cut conditions. *Applied Geophysics*, **16**, 302-313, 2019.
[22] Zhang X, Sun J T, Hu J H et al., "A modified adaptive cross correlation method for flow rate measurement of high-water-cut oil-water flow using planar flowmeter", *IEEE Transactions on Instrumentation and Measurement*, **71**, 9500210, 2022.
[23] Liu C S, Bai L D, Yang Q Y, Jin N D, An improved conductance sensor with inner-outer multi-height ring electrodes for measurement of vertical gas-liquid flow. *IEEE Sensors Journal*, **22**, 6399-6409, 2022.
[24] Zhang W B, Wang C, Wang Y L, "Parameter selection in cross-correlation-based velocimetry using circular electrostatic sensors", *IEEE Transactions on Instrumentation and Measurement*, **59**, 1268-1275, 2010.
[25] Kytömaa H K and Brennen C E, "Small amplitude kinematic wave propagation in two-component media", *International Journal of Multiphase Flow*, **17**, 13-26, 1991.
[26] Lucas G P, Jin N D, "A new kinematic wave model for interpreting cross correlation velocity measurements in vertically upward bubbly oil-in-water flows", *Measurement Science and Technology*, **12**, 1538-1545, 2001.
[27] Maxwell J C A, "A treatise on electricity and magnetism", Clarendon Press, Oxford, 1882.
[28] Zuber N, Findlay J A, "Average volumetric concentration in two-phase flow systems", *International Journal of Heat and Mass Transfer*, **87**, 453-468, 1965.